Software Sensor-Based STATCOM Control Under Unbalanced Conditions

Andres E. Leon, *Student Member, IEEE*, Juan Manuel Mauricio, *Student Member, IEEE*, Jorge A. Solsona, *Senior Member, IEEE*, and Antonio Gomez-Exposito, *Fellow, IEEE*

***Abstract*—A new control strategy for static compensators (STATCOMs) operating under unbalanced voltages and currents is presented in this paper. The proposed strategy adopts a state observer (software sensor) to estimate ac voltages at the STATCOM connection point. This way, physical voltage sensors are not needed and the hardware gets simplified, among other advantages. Using the superposition principle, a controller is designed to independently control both positive and negative sequence currents, eliminating the risk of overcurrents during unbalanced conditions and improving the power quality at the STATCOM connection bus. Two operating modes are proposed for the computation of the reference currents, depending on whether the objective is to compensate unbalanced load currents or regulate bus voltages. The proposed observer allows positive and negative sequences to be estimated in a fraction of the fundamental cycle, avoiding the delay often introduced by filter-based methods. Overall, the STATCOM performance is improved under unbalanced conditions, according to simulation results presented in the paper.**

***Index Terms*—Load compensation, observers, power quality (PQ), sequence currents, software sensors, static compensator (STATCOM), unbalanced systems.**

I. Introduction

THE increased voltage and current capacity of voltage-source converters (VSC), based on self-commutated semiconductors, is leading flexible alternating current transmission systems (FACTS) to naturally arise as a mature yet expensive technology in power systems. Currently, the most frequently used FACTS device is the static compensator (STATCOM), being the most simple, economical, and with a very fast dynamic response. This device, providing several advantages from the electrical network power quality point of view, is being used for reactive power compensation, active power oscillation damping, flicker attenuation, voltage regulation, etc. [1].

Many works have been published up to date about control strategies for STATCOMs. However, conventional controllers present a poorer performance under unbalanced conditions [2]–[5], especially unbalanced voltages, which are relatively common in distribution networks. In addition, converters used in renewable generation applications and high-voltage transmission systems are also frequently required to be capable of overriding unbalanced conditions [6]–[8]. This imbalance could be generated by large unbalanced loads (single-phase electric traction systems, arc furnaces, etc.), or may arise during nearby asymmetrical faults [9].

When a STATCOM is connected to an unbalanced network, a double network frequency $(2\omega_s)$ ripple appears in its dc-bus voltage [10]. When this ripple is not taken into account by the control law, low order harmonics arise in the STATCOM injected currents, deteriorating the situation from the power quality point of view [11]–[13]. In addition, the STATCOM can be considered as a positive-sequence voltage source connected to the grid through a transformer. Therefore, when the grid voltage is not balanced, the STATCOM is a short circuit for the negative-sequence voltages, the negative-sequence currents being only bounded by the transformer reactance. Under these circumstances, the over-current protection may disconnect the STATCOM [2], [5], [11], [14].

Different control strategies have been proposed for the STATCOM. For example, feedback linearization taking currents as outputs was used in [11], [15]–[17], passivity-based controllers were developed in [18], [19], a fuzzy PI-based controller was presented in [1], while in [5] a phasor-based analysis was applied. However, in [15]–[17], [20] the proposed controller lacks the ability to deal with fully unbalanced conditions. In order for the STATCOM to be capable of operating under unbalanced power conditions, while diminishing the risk of overcurrents, it must be able to independently control its positive-sequence and negative-sequence currents. For this reason, a sequence component detection is required. In [5], [11], [14], and [21], phase-locked loops (PLLs) plus filters with a cut-off frequency of $2\omega_s$ are used in order to separate the sequence components. However, such filters generate a delay in the measured signals, reducing the controller bandwidth [14], [22], [23]. To overcome this drawback other techniques have been proposed to estimate the sequences. It is often a practice to use methods based on either discrete Fourier transform (DFT) or Kalman filter. However, these methods present some drawbacks as well. DFT assumes stationary signals and the estimator performance depends on the data window size. A tradeoff exists between estimation speed and noise sensitivity. In order to increase the estimation speed, the windows size should be decreased. However, estimation using small windows is more sensitive to pulsewidth-modulation (PWM) high-frequency

Manuscript received July 17, 2008; revised December 01, 2008. Current version published June 24, 2009. This work was supported in part by the Universidad Nacional del Sur, Consejo Nacional de Investigaciones Científicas y Técnicas (CONICET) and Agencia Nacional de Promoción Científica y Tecnológica (ANPCyT), Argentina, and in part by the Spanish Ministry of Education and Science (MEC) and Junta de Andalucía under ENE2008-68032-C04-02 and P06-TEP-01882, respectively. Paper no. TPWRD-00548-2008.

A. E. Leon and J. A. Solsona are with the Instituto de Investigaciones en Ingeniería Eléctrica (IIIE) "Alfredo Desages" (UNS-CONICET), Departamento de Ingeniería Eléctrica y de Computadoras, Universidad Nacional del Sur (UNS), Bahía Blanca, Argentina (e-mail: aleon@ymail.com; jsolsona@uns.edu.ar).

J. M. Mauricio and A. Gomez-Exposito are with the Department of Electrical Engineering, University of Seville, Seville 41092, Spain (e-mail: j.m.mauricio@ieee.org; age@us.es).

Digital Object Identifier 10.1109/TPWRD.2009.2016810

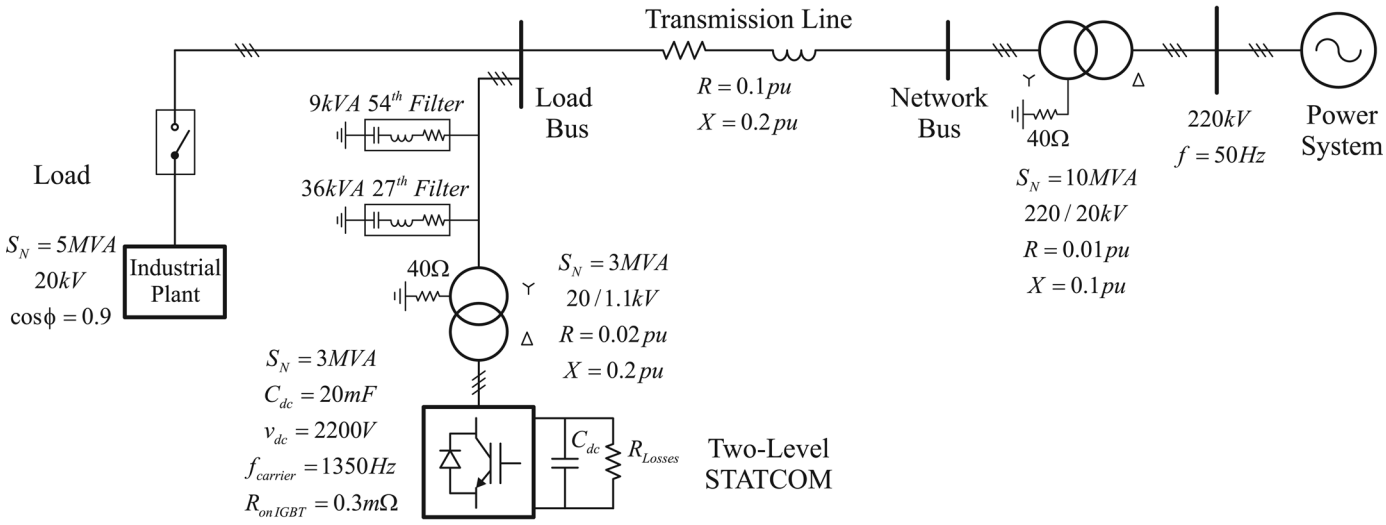

Fig. 1. Power system and STATCOM model.

components appearing in these applications [24]. On the other hand, Kalman filters [25], [26] assume stochastic uncertainties. In this estimator, optimality and speed of convergence depend on the known value of the covariance matrices, among others. Generally, these matrices are unknown and the designer must guess their initial values. For these reasons, in this work state observers based on signal models are proposed to detect the sequence components [27], [28]. This approach improves the estimation of ac current and voltage sequences because the observer is capable of transiently adapting to amplitude variations only in a fraction of the fundamental cycle. In addition, its estimates are obtained without phase delay in steady state.

Besides the issues discussed before for controlling the STATCOM under unbalanced conditions, another important point developed in this work is the ac voltage estimation. In previous articles [1]–[5], [11], [14]–[23], [29], [30], the control strategies require the measurement of ac voltages at the VSC point of connection. In this paper, the ac voltages and their sequence components are estimated from ac current and dc voltage measurements by means of state observers. The use of these observers has several advantages. First, a simplification in the hardware is achieved because ac voltage sensors are not required, saving space, connection cables, high-voltage insulation requirements and, hence, reducing costs. Furthermore, considering the relatively low switching frequency adopted in high power applications, the high level of harmonics present in ac voltages is avoided.

This paper introduces a new control strategy for STATCOMs under unbalanced conditions, capable of independently controlling the positive- and negative-sequence currents. In the proposed implementation ac voltages are estimated via state observers, leading to a simplified and cheaper hardware without ac voltage sensors. The controller design considers two modes of operation, both of them related with quality improvement, namely compensation of unbalanced load currents and regulation of unbalanced bus voltages.

The rest of this paper is organized as follows. Section II presents the system and the STATCOM model. In Section III, the ac voltage observer is designed. In Section IV, the observer-based technique for the computation of current sequences is developed. Section V introduces the proposed control strategy for imbalance compensation. In Section VI, the controller performance evaluation, discussions and tests are presented. Finally, conclusions are drawn in Section VII.

II. System and STATCOM Model

The STATCOM model in the α-β stationary reference frame is given by [31]

$$L\dot{i}_\alpha = -Ri_\alpha + \eta_\alpha v_{\rm dc} - v_\alpha, \tag{1}$$

$$L\dot{i}_\beta = -Ri_\beta + \eta_\beta v_{\rm dc} - v_\beta, \tag{2}$$

$$C_{\rm dc}\dot{v}_{\rm dc} = -\frac{3}{2}\left(\eta_\alpha i_\alpha + \eta_\beta i_\beta\right) - \frac{v_{\rm dc}}{R_L} \tag{3}$$

where i_α, i_β, v_α, and v_β are currents and voltages at the ac side in the $\alpha\beta$ reference frame, η_α and η_β are control signals, and $v_{\rm dc}$ is the dc voltage. The parameters R and L stand for resistance and inductance in the coupling transformer, $C_{\rm dc}$ is the capacitor in the dc-bus, and R_L represents the equivalent converter losses. Note that the equations describing the STATCOM are nonlinear because of the products between control and state variables. Other data and parameters of the considered power system are shown in Fig. 1.

III. AC Voltage Observer Design

In order to estimate the ac voltages at the STATCOM connection point, from the measured currents, a dynamic model is developed for α-β voltages, composed of a positive and a negative sequence

$$v_\alpha = v_\alpha^+ + v_\alpha^-, \tag{4}$$

$$v_\beta = v_\beta^+ + v_\beta^-. \tag{5}$$

In turn, the voltage sequences can be written as a function of their phase angle and magnitude, yielding

$$v_\alpha^+ = v_m^+ \sin\theta^+, \tag{6}$$
$$v_\beta^+ = v_m^+ \cos\theta^+, \tag{7}$$
$$v_\alpha^- = v_m^- \sin\theta^-, \tag{8}$$
$$v_\beta^- = v_m^- \cos\theta^-. \tag{9}$$

Differentiating (6)–(9) gives

$$\dot{v}_\alpha^+ = \omega_s v_\beta^+, \tag{10}$$
$$\dot{v}_\beta^+ = -\omega_s v_\alpha^+, \tag{11}$$
$$\dot{v}_\alpha^- = -\omega_s v_\beta^-, \tag{12}$$
$$\dot{v}_\beta^- = \omega_s v_\alpha^- \tag{13}$$

where the sequences are considered to rotate in the opposite direction ($\dot{\theta}^+ = \omega_s, \dot{\theta}^- = -\omega_s$), and their magnitudes are assumed to be slowly time varying.

In what follows, the design of a reduced-order observer with linear error dynamics used for estimating v_α^+, v_β^+, v_α^-, and v_β^- is introduced. Note that the dynamics of both STATCOM currents (1) and (2) and ac voltages (10)–(13) can be partitioned in two subsystems, resulting in

$$\dot{\mathbf{x}}_a = \mathbf{N}\mathbf{x}_a + \mathbf{C}\mathbf{x}_b + \mathbf{g}_a, \tag{14}$$
$$\dot{\mathbf{x}}_b = \mathbf{R}\mathbf{x}_a + \mathbf{S}\mathbf{x}_b + \mathbf{g}_b \tag{15}$$

where $\mathbf{x}_a = [i_\alpha \; i_\beta]^T$ is the vector of measured states, $\mathbf{x}_b = [v_\alpha^+ \; v_\beta^+ \; v_\alpha^- \; v_\beta^-]^T$ comprises the states to be estimated and the involved matrices are given by

$$\mathbf{N} \triangleq \begin{bmatrix} -\frac{R}{L} & 0 \\ 0 & -\frac{R}{L} \end{bmatrix}, \quad \mathbf{C} \triangleq \begin{bmatrix} -\frac{1}{L} & 0 & -\frac{1}{L} & 0 \\ 0 & -\frac{1}{L} & 0 & -\frac{1}{L} \end{bmatrix},$$
$$\mathbf{R} \triangleq \mathbf{0}^{4\times 2},$$
$$\mathbf{S} \triangleq \begin{bmatrix} 0 & \omega_s & 0 & 0 \\ -\omega_s & 0 & 0 & 0 \\ 0 & 0 & 0 & -\omega_s \\ 0 & 0 & \omega_s & 0 \end{bmatrix}, \quad \mathbf{g}_a \triangleq \begin{bmatrix} \frac{\eta_\alpha v_{\mathrm{dc}}}{L} \\ \frac{\eta_\beta v_{\mathrm{dc}}}{L} \end{bmatrix},$$
$$\mathbf{g}_b \triangleq \mathbf{0}^{4\times 1}. \tag{16}$$

For convenience, (14) can be rearranged as follows:

$$\underbrace{\dot{\mathbf{x}}_a - (\mathbf{N}\mathbf{x}_a + \mathbf{g}_a)}_{\mathbf{y}} = \mathbf{C}\mathbf{x}_b. \tag{17}$$

The resulting system, composed of (15) and (17), describes the dynamics of the unmeasured variables $\mathbf{x}_b$ and the output equation of the new subsystem ($\mathbf{y} = \mathbf{C}\mathbf{x}_b$), respectively. For this formulation, a Luenberger-like reduced-order observer is given by [32]

$$\dot{\hat{\mathbf{x}}}_b = \underbrace{\mathbf{S}\hat{\mathbf{x}}_b + \mathbf{R}\mathbf{x}_a + \mathbf{g}_b}_{\text{prediction term}} + \underbrace{\mathbf{G}\,(\mathbf{y} - \mathbf{C}\hat{\mathbf{x}}_b)}_{\text{correction term}}. \tag{18}$$

The correction term keeps the convergence rate under control of the estimation error, allowing parametric uncertainties and non-modeled dynamics appearing in the prediction term to be rejected. This is a very interesting feature of the closed-loop estimator, because robustness is increased. Uncertainty attenuation is directly proportional to the norm of the correction term gain matrix ($\mathbf{G}$). Nevertheless, the maximum value of the $\mathbf{G}$ norm to be chosen is bounded by the measurement noise. It is worth noting also that the estimation of $\mathbf{x}_b$ involves the time derivative of $\mathbf{x}_a$. In order to prevent the amplification of noise originating in the differentiation of the measured variable, the following transformation is used $\boldsymbol{\xi} = \hat{\mathbf{x}}_b - \mathbf{G}\mathbf{x}_a$. Then, rewriting (18) in terms of $\boldsymbol{\xi}$, the following structure to be implemented results:

$$\dot{\boldsymbol{\xi}} = \mathbf{A}_r(\boldsymbol{\xi} + \mathbf{G}\mathbf{x}_a) + \mathbf{B}_r, \tag{19}$$
$$\hat{\mathbf{x}}_b = \boldsymbol{\xi} + \mathbf{G}\mathbf{x}_a \tag{20}$$

where the time-derivative of $\mathbf{x}_a$ is not required and the following matrices have been introduced:

$$\mathbf{A}_r \triangleq \mathbf{S} - \mathbf{G}\mathbf{C}, \tag{21}$$
$$\mathbf{B}_r \triangleq -\mathbf{G}(\mathbf{N}\mathbf{x}_a + \mathbf{g}_a). \tag{22}$$

The estimation error ($\mathbf{e} = \mathbf{x}_b - \hat{\mathbf{x}}_b$) dynamics is obtained by subtracting (18) from (15)

$$\dot{\mathbf{e}} = \dot{\mathbf{x}}_b - \dot{\hat{\mathbf{x}}}_b = (\mathbf{S} - \mathbf{G}\mathbf{C})(\mathbf{x}_b - \hat{\mathbf{x}}_b) = \mathbf{A}_r\mathbf{e}. \tag{23}$$

Note that the error dynamics become linear and, consequently, linear techniques can be used for tuning the observer, such as pole assignment, linear quadratic regulation (LQR), etc. In this way, the observer gain matrix $\mathbf{G}$ can be easily calculated to obtain a fast convergence rate. Therefore, as will be shown, good estimates in a small cycle fraction are attained.

Expressions given by (19) and (20), when expanded to the STATCOM particular case, result in the following observer:

$$\dot{\xi}_1 = \frac{a_1 g_1 - a_2 g_2 + c b_1 + (g_2\eta_\beta - g_1\eta_\alpha)v_{\mathrm{dc}}}{L} + (\xi_2 + b_2)\omega_s, \tag{24}$$
$$\dot{\xi}_2 = \frac{a_2 g_1 + a_1 g_2 + c b_2 - (g_1\eta_\beta + g_2\eta_\alpha)v_{\mathrm{dc}}}{L} - (\xi_1 + b_1)\omega_s, \tag{25}$$
$$\dot{\xi}_3 = \frac{a_1 g_1 + a_2 g_2 + c b_3 - (g_1\eta_\alpha + g_2\eta_\beta)v_{\mathrm{dc}}}{L} - (\xi_4 + b_4)\omega_s, \tag{26}$$
$$\dot{\xi}_4 = \frac{a_2 g_1 - a_1 g_2 + c b_4 + (g_2\eta_\alpha - g_1\eta_\beta)v_{\mathrm{dc}}}{L} + (\xi_3 + b_3)\omega_s \tag{27}$$

with

$$\hat{v}_\alpha^+ = \xi_1 + g_1 i_\alpha - g_2 i_\beta, \tag{28}$$
$$\hat{v}_\beta^+ = \xi_2 + g_2 i_\alpha + g_1 i_\beta, \tag{29}$$
$$\hat{v}_\alpha^- = \xi_3 + g_1 i_\alpha + g_2 i_\beta, \tag{30}$$
$$\hat{v}_\beta^- = \xi_4 + g_1 i_\beta - g_2 i_\alpha, \tag{31}$$

and

$$a_1 \triangleq \xi_1 + \xi_3, \quad a_2 \triangleq \xi_2 + \xi_4, \quad b_1 \triangleq g_1 i_\alpha - g_2 i_\beta,$$
$$b_2 \triangleq g_2 i_\alpha + g_1 i_\beta, \quad b_3 \triangleq g_1 i_\alpha + g_2 i_\beta,$$
$$b_4 \triangleq g_1 i_\beta - g_2 i_\alpha, \quad c \triangleq 2g_1 + R$$

where the scalars g_1 and g_2 are entries of the gain matrix $\mathbf{G}$. Note that the observer expressions given by (24)–(31) are simple enough to be implemented in commercially available digital signal processors (DSPs).

The observer initial state conditions can be computed beforehand during the STATCOM start-up process, in order to reduce the initial transient error. In [33] and [34], some strategies to deal with this requirement during the observer initialization phase are given.

IV. AC Current Observer Design

In this section, the observer aimed at estimating positive- and negative-sequence components of STATCOM currents, measured at the ac side, is described. This observer will be used in the next section where the observer-based controller will be designed. In general, an unbalanced three-phase current without a zero-sequence component can be decomposed as

$$i_\alpha = i_\alpha^+ + i_\alpha^-, \tag{32}$$
$$i_\beta = i_\beta^+ + i_\beta^-. \tag{33}$$

Similar to the ac voltage case (10)–(13), a dynamic model for the ac currents composed of two components (positive and negative sequences), rotating in the opposite direction, can be written as follows:

$$\dot{i}_\alpha^+ = \omega_s i_\beta^+, \tag{34}$$
$$\dot{i}_\beta^+ = -\omega_s i_\alpha^+, \tag{35}$$
$$\dot{i}_\alpha^- = -\omega_s i_\beta^-, \tag{36}$$
$$\dot{i}_\beta^- = \omega_s i_\alpha^-. \tag{37}$$

The set of equations just shown constitutes a dynamic linear system, with the currents i_α and i_β as measurable outputs. In compact form, it can be expressed as

$$\dot{\mathbf{x}} = \mathbf{A}\mathbf{x}, \tag{38}$$
$$\mathbf{y} = \mathbf{C}\mathbf{x} \tag{39}$$

where the following components have been defined:

$$\mathbf{x} = [i_\alpha^+ \quad i_\beta^+ \quad i_\alpha^- \quad i_\beta^-]^T, \quad \mathbf{y} = [i_\alpha \quad i_\beta]^T,$$
$$\mathbf{A} = \begin{bmatrix} 0 & \omega_s & 0 & 0 \\ -\omega_s & 0 & 0 & 0 \\ 0 & 0 & 0 & -\omega_s \\ 0 & 0 & \omega_s & 0 \end{bmatrix}, \quad \mathbf{C} = \begin{bmatrix} 1 & 0 & 1 & 0 \\ 0 & 1 & 0 & 1 \end{bmatrix}. \tag{40}$$

Therefore, in this case, a linear observer can be implemented to estimate the states $[i_\alpha^+ \ i_\beta^+ \ i_\alpha^- \ i_\beta^-]$ as follows:

$$\dot{\hat{\mathbf{x}}} = \mathbf{A}\hat{\mathbf{x}} + \mathbf{G}(\mathbf{y} - \mathbf{C}\hat{\mathbf{x}}). \tag{41}$$

The estimation error dynamics $\mathbf{e} \triangleq \mathbf{x} - \hat{\mathbf{x}}$ are given by subtracting (41) from (38)

$$\dot{\mathbf{e}} = (\mathbf{A} - \mathbf{G}\mathbf{C})\mathbf{e}. \tag{42}$$

The gain matrix $\mathbf{G}$ is designed to keep the convergence rate of the estimation error under control. In this paper, the eigenvalues of the matrix characterizing the estimation error dynamics (42) are determined by means of an LQR optimization process. This yields $\lambda_i = -\sqrt{3}\omega_s$, leading to an estimation time constant of $\tau = 1.83$ ms. Consequently, after a time of 3τ (5.5 ms), the estimation error will be lower than 5%, which means that perturbations of the current sequence components will be estimated in approximately 1/4 of a cycle.

Note that the estimation error dynamics (42) are equivalent to that of the ac voltage observer (23). Hence, both designs are implemented in a similar manner, the same speed of response is obtained for the estimation of currents and voltages, even though the latter are not measured.

V. Feedback Linearization Control Strategy

A. Decoupled Current Control

In order to compensate unbalanced load power, independent control of the positive and negative sequences of the STATCOM-injected currents are required. For this purpose, the following auxiliary variables are defined:

$$e_\alpha \triangleq \eta_\alpha v_{\mathrm{dc}}, \tag{43}$$
$$e_\beta \triangleq \eta_\beta v_{\mathrm{dc}}. \tag{44}$$

Taking into account (43) and (44), the STATCOM current dynamics (1) and (2) become linear. Therefore, assuming that parameters R and L are the same for each phase, the superposition theorem can be applied by splitting the positive and negative effects, yielding

$$L\dot{i}_\alpha^+ = -Ri_\alpha^+ + e_\alpha^+ - v_\alpha^+, \tag{45}$$
$$L\dot{i}_\beta^+ = -Ri_\beta^+ + e_\beta^+ - v_\beta^+, \tag{46}$$
$$L\dot{i}_\alpha^- = -Ri_\alpha^- + e_\alpha^- - v_\alpha^-, \tag{47}$$
$$L\dot{i}_\beta^- = -Ri_\beta^- + e_\beta^- - v_\beta^-. \tag{48}$$

A similar approach, in a d–q reference frame, is developed in [2], [3], [10], [11], and [35].

Then, the auxiliary variables can be defined as follows:

$$e_\alpha^+ = Ri_\alpha^+ + v_\alpha^+ + Lu_\alpha^+, \tag{49}$$
$$e_\beta^+ = Ri_\beta^+ + v_\beta^+ + Lu_\beta^+, \tag{50}$$
$$e_\alpha^- = Ri_\alpha^- + v_\alpha^- + Lu_\alpha^-, \tag{51}$$
$$e_\beta^- = Ri_\beta^- + v_\beta^- + Lu_\beta^-, \tag{52}$$

and keep in mind that (49)–(52) and (45)–(48) reduce to

$$\dot{i}_\alpha^+ = u_\alpha^+, \tag{53}$$
$$\dot{i}_\beta^+ = u_\beta^+, \tag{54}$$
$$\dot{i}_\alpha^- = u_\alpha^-, \tag{55}$$
$$\dot{i}_\beta^- = u_\beta^-. \tag{56}$$

The important observation is that with this method, the dynamics of the four currents i_α^+, i_β^+, i_α^-, and i_β^- are written as

decoupled linear systems. Therefore, linear control strategies can be applied to control them independently.

Note also that the systems (53)–(56) adopt the general form $\dot{i} = u$. If the current tracking error is defined as $\tilde{i} \triangleq i - i^\star$, then the following tracking error dynamics $\dot{\tilde{i}} + k_p\tilde{i} = 0$ can be proposed, from which the auxiliary input u can be obtained:

$$u = \dot{i}^\star - k_p(i - i^\star). \tag{57}$$

In the sequel, the superscript "$\star$" denotes the desired reference values. Then, the four auxiliary control inputs u_α^+, u_β^+, u_α^-, and u_β^- can be obtained from the general expression (57), yielding

$$u_\alpha^+ = \omega_s i_\beta^{+\star} - k_p(i_\alpha^+ - i_\alpha^{+\star}), \tag{58}$$
$$u_\beta^+ = -\omega_s i_\alpha^{+\star} - k_p(i_\beta^+ - i_\beta^{+\star}), \tag{59}$$
$$u_\alpha^- = -\omega_s i_\beta^{-\star} - k_p(i_\alpha^- - i_\alpha^{-\star}), \tag{60}$$
$$u_\beta^- = \omega_s i_\alpha^{-\star} - k_p(i_\beta^- - i_\beta^{-\star}), \tag{61}$$

where, for the current time-derivatives, (34)–(37) should be used. Note that (58)–(61) involves the individual sequence components of the STATCOM currents, which are provided by the observer designed in the previous section.

Finally, the original inputs η_α and η_β are obtained from (43) and (44), using (49)–(52), leading to

$$\eta_\alpha = \frac{e_\alpha^+ + e_\alpha^-}{v_{\rm dc}} = \frac{1}{v_{\rm dc}}(Ri_\alpha + v_\alpha + L(u_\alpha^+ + u_\alpha^-)), \tag{62}$$
$$\eta_\beta = \frac{e_\beta^+ + e_\beta^-}{v_{\rm dc}} = \frac{1}{v_{\rm dc}}(Ri_\beta + v_\beta + L(u_\beta^+ + u_\beta^-)). \tag{63}$$

The control laws (62) and (63) are nonlinear, owing to the presence of $v_{\rm dc}$ in the denominator. However, this allows dc voltage variations to be compensated in an attempt to reduce the presence of low-order harmonics in the STATCOM currents. As explained before, these harmonics are generated by a dc voltage ripple of frequency $2\omega_s$, arising during unbalanced grid conditions.

The proposed strategy is a nonlinear law where the estimates provided by an observer are included. In the linear case, the closed-loop stability (observer-based controller plus plant) is guaranteed by using the Separation Theorem [32]. Consequently, the control law and observer convergence rate can be fixed independently. Since the Separation Theorem does not apply in the nonlinear case, when choosing the observer gains, some conditions should be considered to guarantee stability. Some research establishes sufficient conditions to guarantee asymptotic convergence in the nonlinear case (see, for instance, [36]–[38]). In our case, the observer can be designed as follows: the nonlinear control strategy is calculated by assuming that the true states are available; then, observer gains are selected by satisfying the sufficient conditions presented in [39]. These conditions establish how fast the observer convergence must be to guarantee closed-loop stability.

B. DC Voltage Control

For the correct STATCOM operation, considering the internal and switching losses, a dc voltage-control loop is implemented through the positive-sequence active power p_c^+, consumed by the STATCOM. This control is implemented with a PI loop as follows:

$$p_c^{+\star}(s) = \frac{k_{dcp}s + k_{dci}}{s(T_a s + 1)^2}(v_{\rm dc} - v_{\rm dc}^\star)(s). \tag{64}$$

Under unbalanced conditions, a $2\omega_s$ ripple frequency appears in the dc bus voltage. This ripple should be filtered out in order to prevent distortion in the STATCOM-injected currents. By using the time constant T_a of the controller (64), it is possible to calculate the cutoff frequency for filtering purposes [11], [19], [21]. In this way, the STATCOM positive-sequence active power is not distorted.

C. Reactive Power Injection and AC Voltage Amplitude Control

In order to determine the positive-sequence reference for the reactive power ($q_c^{+\star}$), three situations can be considered.

1) ▷ A fixed amount of reactive power must be injected by the STATCOM for network support (according to the power system operator settings).
2) ▷ Calculate to compensate for the load reactive power (e.g., to satisfy the unity power factor condition).
3) ▷ The STATCOM tries to keep a desired ac voltage (v_C) at the connection point.

In the first two cases, the reactive power reference is provided externally by the system operator or computed to satisfy the required power factor. In the third case, the power reference can be computed through the following voltage-control scheme [15], [17]:

$$q_c^{+\star} = -k_{vcp}(v_C - v_C^\star) - k_{vci}\int (v_C - v_C^\star)dt. \tag{65}$$

In the block diagram of Fig. 2, these control modes are chosen by the selector S_1.

D. Positive-Sequence Current References

From the positive sequence of the desired active and reactive powers, the STATCOM positive-sequence current references can be calculated by using the instantaneous active and reactive power theory [40] as follows:

$$i_\alpha^{+\star} = \frac{2}{3}\frac{p_c^{+\star}v_\alpha^+ - q_c^{+\star}v_\beta^+}{v_\alpha^{+2} + v_\beta^{+2}}, \tag{66}$$
$$i_\beta^{+\star} = \frac{2}{3}\frac{q_c^{+\star}v_\alpha^+ + p_c^{+\star}v_\beta^+}{v_\alpha^{+2} + v_\beta^{+2}} \tag{67}$$

where only the positive-sequence component of the voltage is considered, as it is desired that $p_c^{+\star}$ and $q_c^{+\star}$ are injected through positive-sequence currents. The injection of negative-sequence currents is discussed in the next subsection.

E. Negative-Sequence Current References

Two operating modes for the STATCOM will be considered. In the first mode, the STATCOM is used to compensate load current imbalances. The goal is to let the grid "see" a balanced

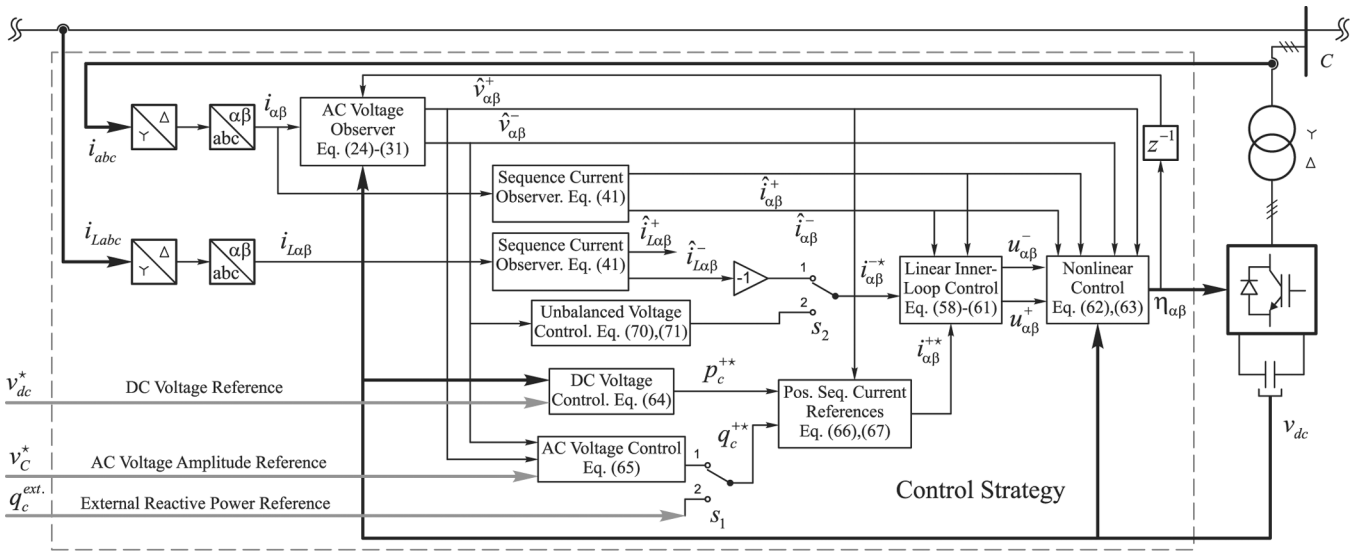

Fig. 2. Block diagram for the proposed control strategy.

load and, consequently, to prevent unbalanced voltage drops that deteriorate PQ indices. In the second mode, the objective of the STATCOM is to directly compensate the voltage imbalance at the connection point. Unbalanced voltages may be a consequence of close unbalanced loads or asymmetrical faults in the power system. This is an important feature of the proposed approach considering that some loads are very sensitive to unbalanced voltages. Both operating modes are chosen by the selector S_2 (see Fig. 2).

As explained before, in the first operating mode, the STATCOM has to get rid of negative-sequence load currents. Therefore, the references to be tracked are

$$i_{\alpha}^{-\star} = -i_{L\alpha}^{-}, \tag{68}$$

$$i_{\beta}^{-\star} = -i_{L\beta}^{-} \tag{69}$$

where the observer described in Section IV can be used to obtain the negative-sequence component of the load current ($i_{L\alpha}^{-}$ and $i_{L\beta}^{-}$).

When the converter is connected to an unbalanced voltage, its negative-sequence component sees the STATCOM as a short circuit. As a consequence, the negative-sequence currents are only limited by the STATCOM transformer impedance, which may lead to overcurrents. The proposed strategy can be also tailored to protect the STATCOM against such overcurrents, by setting the negative-sequence current to zero (for instance $i_{\alpha}^{-\star} = i_{\beta}^{-\star} = 0$).

In the second operating mode, the STATCOM uses the negative-sequence current controller to reduce the voltage imbalance. The negative-sequence current references are obtained from the following control loops:

$$i_{\alpha}^{-\star} = -k_{vp}(v_{\alpha}^{-} - v_{\alpha}^{-\star}) - k_{vi}\int (v_{\alpha}^{-} - v_{\alpha}^{-\star})dt, \tag{70}$$

$$i_{\beta}^{-\star} = -k_{vp}(v_{\beta}^{-} - v_{\beta}^{-\star}) - k_{vi}\int (v_{\beta}^{-} - v_{\beta}^{-\star})dt. \tag{71}$$

In order to minimize the negative-sequence voltages, references $v_{\alpha}^{-\star}$ and $v_{\beta}^{-\star}$ are set to zero. In this mode, the load bus voltages are balanced because of the voltage drops originated by the negative-sequence STATCOM currents, when circulating through the network equivalent impedance. However, if the impedance between the unbalanced power grid and the load is small (high short-circuit power), very large currents are needed to balance the bus voltages, which may saturate the STATCOM current capability.

VI. Performance Testing

This section presents the most relevant results regarding the assessment of the proposed controller. The system, STATCOM, and control strategy are implemented via the SimPowerSystems blockset of SIMULINK/MATLAB. Controller gains are set to $k_p = 800\ \mathrm{s}^{-1}$, $k_{dcp} = 2\ \mathrm{kWV}^{-1}$, $k_{dci} = 60\ \mathrm{kWV}^{-1}\mathrm{s}^{-1}$, $T_a = 3.18$ ms, $k_{vcp} = 2\ \mathrm{kWV}^{-1}$, $k_{vci} = 25\ \mathrm{kWV}^{-1}\mathrm{s}^{-1}$, $k_{vp} = 100\ \Omega^{-1}$, and $k_{vi} = 3000\ \Omega^{-1}\mathrm{s}^{-1}$, whereas observer gains are $g_1 = \sqrt{3}\omega_s$, and $g_2 = \omega_s$. Other data and parameters are provided in the one-line electrical diagram of Fig. 1. To obtain a digital controller, the Euler rule is employed to convert continuous time equations to the discrete-time domain $\dot{x} \cong (x_{k+1} - x_k)/(h)$, where h is the sample time (set to 50 μs for the experiments that will be reported).

A. Biphase Fault on the Load Side

In the first test, the controller performance when compensating unbalanced load currents is analyzed. To this end, a 110 ms biphase fault on the load side, leading to positive- and negative-sequence currents during the fault period, is considered, as illustrated in Fig. 3(a). Estimates of the current sequences are shown in Fig. 3(b) and (c), respectively, where the resulting estimation time is only a fraction of the fundamental cycle. This is an important feature of the proposed control technique, because these estimates are used in the control law for obtaining fast and accurate compensation. In Fig. 3(d), the currents provided by the network equivalent are depicted, remaining balanced every time. The currents injected by the STATCOM, mainly containing a negative-sequence component (acb) that compensates the imbalance caused by the fault, are

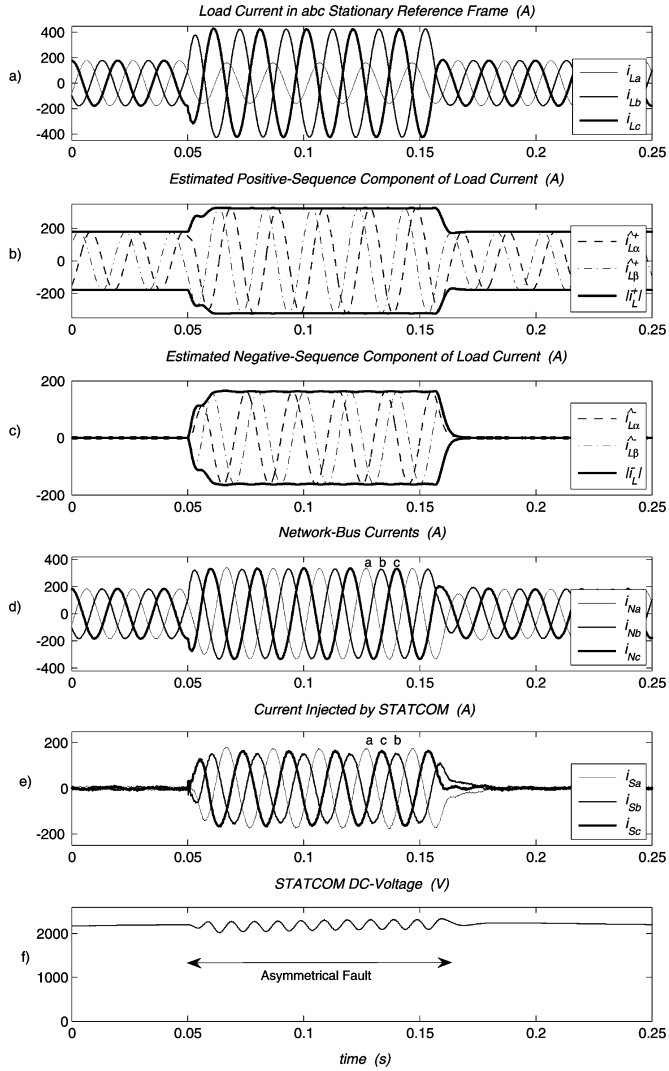

Fig. 3. Compensation of a biphase fault on the load side.

illustrated in Fig. 3(e). Finally, Fig. 3(f) shows the STATCOM dc bus voltage, containing a ripple during the fault period whose frequency doubles the fundamental one.

B. Simultaneous Voltage and Current Imbalance

In this second experiment, the STATCOM operating in the unbalanced current compensation mode $(S_2 = 1)$ is tested. The system is balanced when at $t = 0.05$ s, an asymmetric fault occurs on the power system side, giving rise to an unbalanced voltage at the load bus [see Fig. 4(a)]. Therefore, after $t = 0.05$ s, the load absorbs an unbalanced current [Fig. 4(b)]. This unbalanced condition is rapidly detected and compensated by the STATCOM, in such a way that balanced currents are provided by the external system [see Fig. 4(c)]. Then, at $t = 0.15$ s, a single load phase becomes disconnected, while the unbalanced network condition remains. In these strongly unbalanced conditions, the load consumes a highly unbalanced current [see Fig. 4(b), after $t = 0.15$ s]. Despite that, the power system sees a balanced condition because of the STATCOM reaction [see

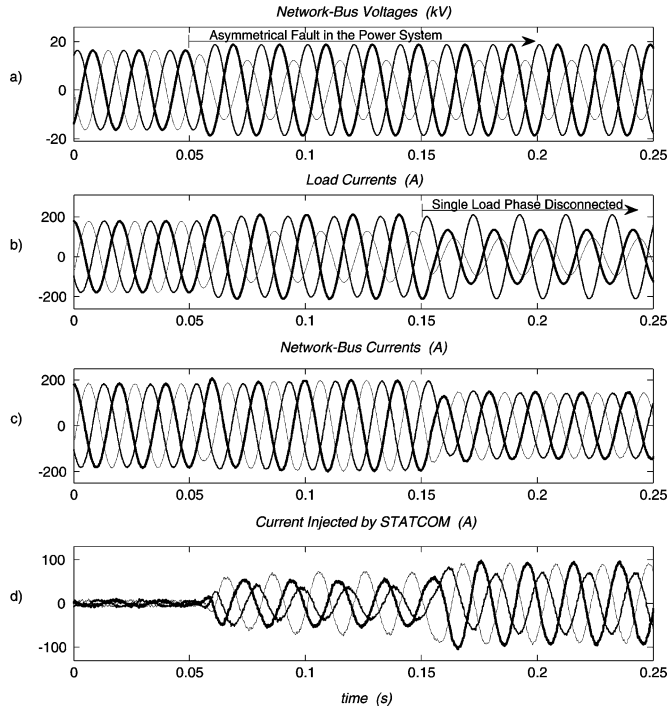

Fig. 4. Behavior against voltage and current asymmetrical faults.

Fig. 4(c)]. The currents injected by the STATCOM are depicted in Fig. 4(d).

C. Unbalanced Load Current and Power Factor Correction

This test is aimed at studying the behavior of the controller when compensating unbalanced load currents and reactive power simultaneously. In Fig. 5(a) and (b), load currents and bus voltages are plotted, respectively, both of them being unbalanced. Fig. 5(c) shows the current injected by the STATCOM in this condition. At $t = 0.1$ s, the controller injects reactive power to improve the load power factor $(S_1 = 2)$. As can be seen, even though currents and voltages are unbalanced, the converter injects balanced reactive currents, showing the capability of the controller to deal with unbalanced conditions. Then, at $t = 0.17$ s, the control mode oriented to balance load currents is also activated $(S_2 = 1)$. Fig. 5(d) shows that the currents absorbed from the power system are totally balanced after a fraction of a cycle. In addition, the controller performance in regulating the dc bus voltage can be observed in Fig. 5(e).

In Fig. 5(f), the actual ac voltage and the estimated positive- and negative-sequence components at the load bus are plotted. Note that due to the insulated-gate bipolar transistors (IGBTs) low switching frequency, typical in these high-power applications, the actual ac voltage contains high-order harmonics. On the other hand, the estimated voltages are much softer, with less harmonics content [see a zoomed view in Fig. 5(f)]. Moreover, unlike the traditional filter-based methods, there is no phase lag in the estimated voltages when the proposed observer is used. Another important feature of the proposed controller is that positive and negative sequences are estimated in a fraction of the fundamental cycle, reducing the usually longer delay associated with other techniques. Shorter delays help reject disturbances and compensate both grid and load imbalances in a faster way.

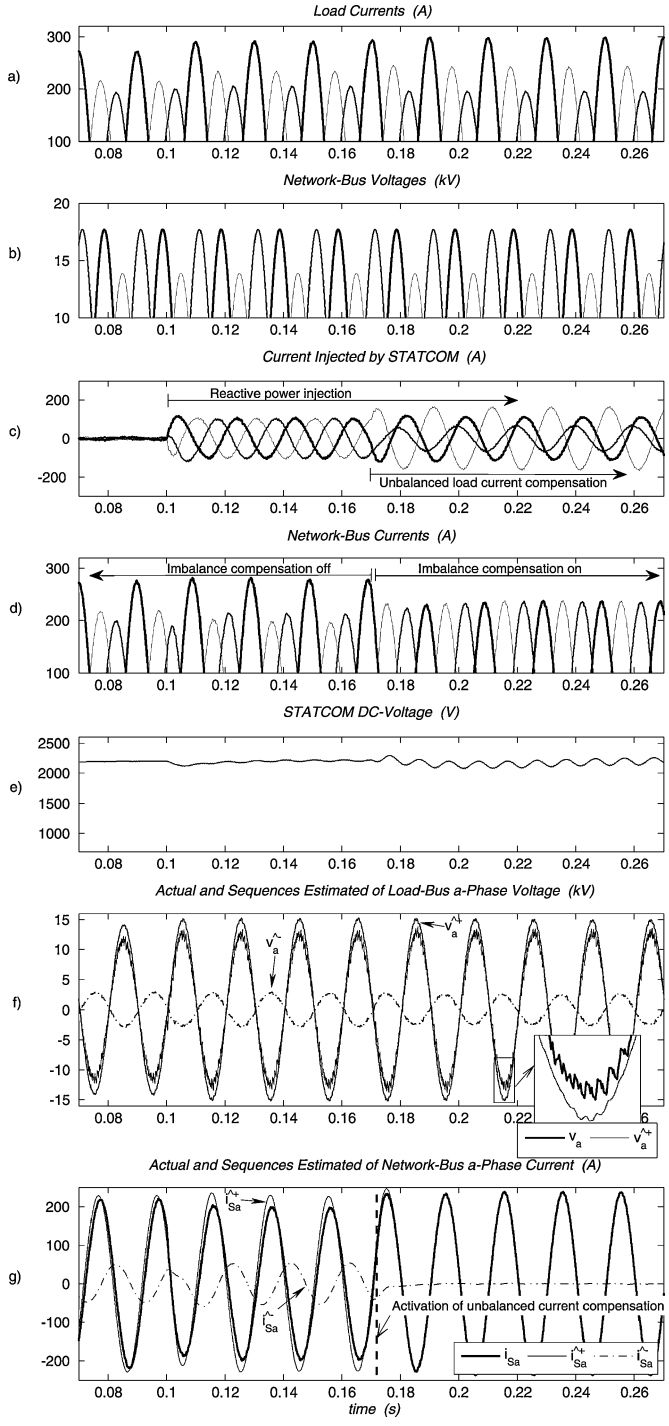

Fig. 5. Unbalanced load current compensation control mode.

Finally, Fig. 5(g) shows the actual current provided by the network, along with its estimated sequences. Before the current balancing control is activated ($t < 0.17$ s), the current provided by the power system contains a negative-sequence component, which is completely eliminated afterwards ($t > 0.17$ s).

D. Unbalanced Voltage Compensation

This test tries to assess the STATCOM capability to compensate unbalanced voltages ($S_2 = 2$). An asymmetrical fault at $t = 0.1$ s on the external system side, lasting for 100 ms, gives rise

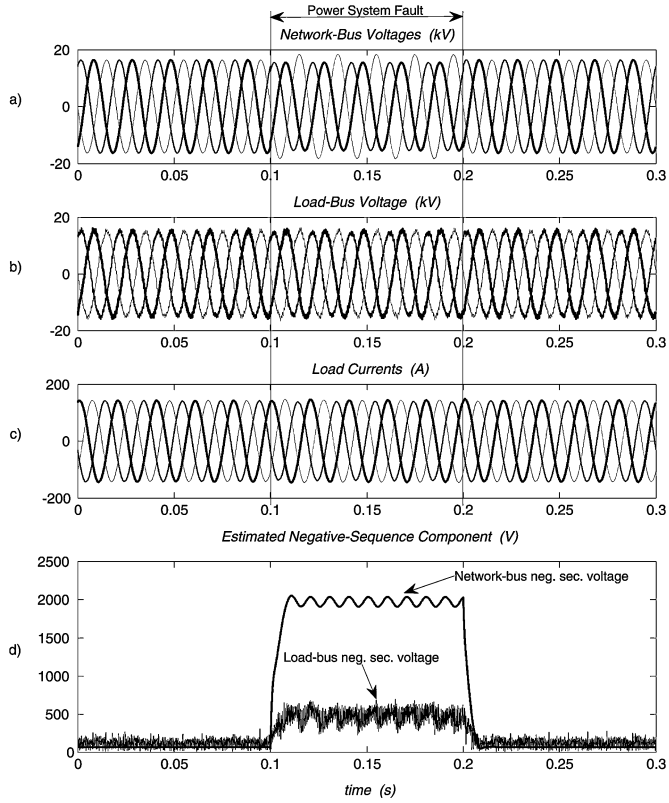

Fig. 6. STATCOM improving the load bus voltage imbalance.

to unbalanced voltages at the load bus, as shown in Fig. 6(a). The STATCOM reacts immediately to reduce the load voltage and load current imbalances [see Fig. 6(b) and (c)]. Fig. 6(d) represents the estimated negative-sequence voltage, both at the load and network buses. As can be seen, a 2 kV negative-sequence component arises at the network bus voltage, which is reduced by the STATCOM to about 500 V at the load bus. In this case, owing to the short-circuit power assumed, the STATCOM reaches its rated power, which explains the remaining voltage imbalance at the load bus.

E. Unbalanced Voltage Compensation and Voltage Regulation

In this last test, the ability of the STATCOM to compensate voltage imbalances and, at the same time, regulate the voltage magnitude is checked. Fig. 7(a)–(c) shows the load currents and the voltages at the network and load buses, respectively, which are all unbalanced in this experiment. Upon activation of the imbalance compensation control, at $t = 0.13$ s ($S_2 = 2$), the load bus voltage is significantly balanced, as can be seen in Fig. 7(e), where the negative-sequence component of such a voltage is shown. Then, the positive-sequence voltage regulation control is activated at $t = 0.2$ s ($S_1 = 1$), yielding a 5% reduction of the voltage drop, as shown in Fig. 7(d). The fact that the negative sequence component is not totally compensated in this case is explained by the STATCOM reaching its rated power limit at this level of compensation.

VII. Conclusion

A new software sensor-based control strategy is presented in this paper, allowing STATCOM devices to operate under un-

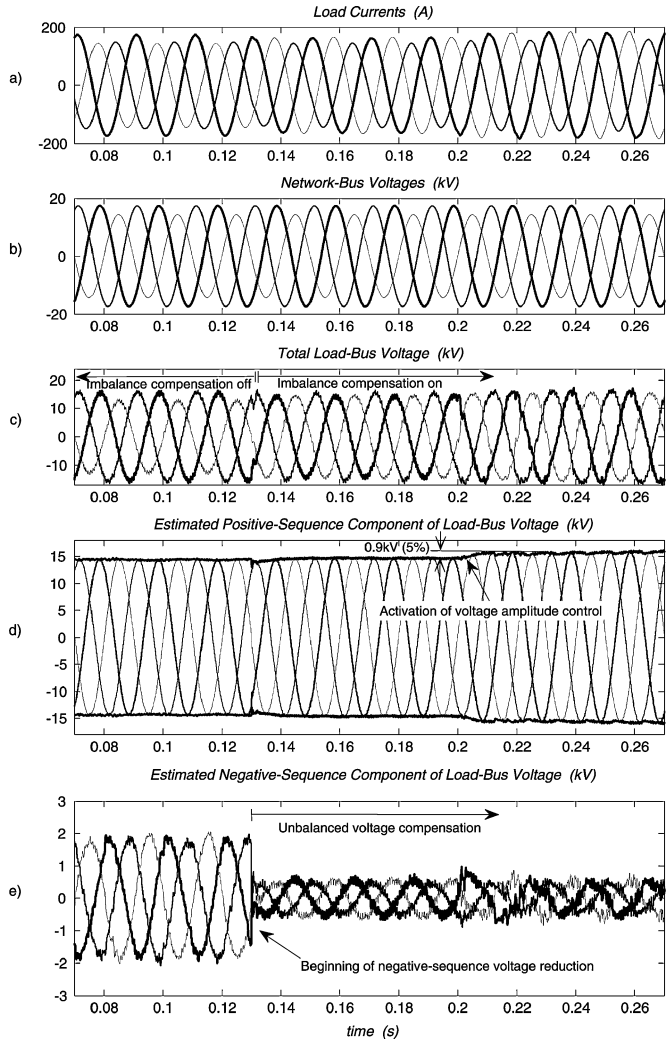

Fig. 7. Unbalanced voltage compensation control mode.

balanced power grid conditions in a satisfactory manner. The controller design is based on the decomposition of voltages and currents into their sequence components. This makes it possible to avoid low-order harmonics in the STATCOM currents and to reduce the outage risk associated with overcurrents appearing under unbalanced conditions.

Furthermore, by using the proposed strategy, the required hardware can be reduced, since ac voltage sensors are not needed. Consequently, cost is decreased and reliability is enhanced. The proposed controller has two operating modes aimed at compensating unbalanced currents and improving voltage regulation, respectively.

The ever-increasing PQ requirements make the proposed controller an attractive choice for industrial plants. Other application fields could be found in sensitive loads that are close to large unbalanced loads in relatively weak areas of an electric network, where the PQ must be enhanced.

REFERENCES

[1] B. N. Singh, A. Chandra, and K. Al-Haddad, "DSP-based indirect-current-controlled STATCOM. Part II: Multifunctional capabilities," *Proc. Inst. Elect. Eng., Elect. Power Appl.*, vol. 147, pp. 113–118, Mar. 2000.

[2] B. Blazic and I. Papic, "Improved D-StatCom control for operation with unbalanced currents and voltages," *IEEE Trans. Power Del.*, vol. 21, no. 1, pp. 225–233, Jan. 2006.

[3] M. Bongiorno and J. Svensson, "Voltage dip mitigation using shunt-connected voltage source converter," *IEEE Trans. Power Electron.*, vol. 22, no. 5, pp. 1867–1874, Sep. 2007.

[4] C. A. C. Cavaliere, E. H. Watanabe, and M. Aredes, "Multi-pulse STATCOM operation under unbalanced voltages," in *Proc. IEEE Power Eng. Soc. Winter Meeting*, Jan. 2002, vol. 1, pp. 567–572.

[5] K. Li, J. Liu, Z. Wang, and B. Wei, "Strategies and operating point optimization of STATCOM control for voltage unbalance mitigation in three-phase three-wire systems," *IEEE Trans. Power Del.*, vol. 22, no. 1, pp. 413–422, Jan. 2007.

[6] M. Hagiwara, K. Wada, H. Fujita, and H. Akagi, "Dynamic behavior of a 21-level BTB-based power-flow controller under single-line-to-ground fault conditions," *IEEE Trans. Ind. Appl.*, vol. 43, no. 5, pp. 1379–1387, Sep../Oct. 2007.

[7] L. Xu and Y. Wang, "Dynamic modeling and control of DFIG-based wind turbines under unbalanced network conditions," *IEEE Trans. Power Syst.*, vol. 22, no. 1, pp. 314–323, Feb. 2007.

[8] C. H. Ng, L. Ran, and J. Bumby, "Unbalanced-grid-fault ride-through control for a wind turbine inverter," *IEEE Trans. Ind. Appl.*, vol. 44, no. 3, pp. 845–856, May/Jun. 2008.

[9] A. von Jouanne and B. Banerjee, "Assessment of voltage unbalance," *IEEE Trans. Power Del.*, vol. 16, no. 4, pp. 782–790, Oct. 2001.

[10] P. Rioual, H. Pouliquen, and J.-P. Louis, "Regulation of a pwm rectifier in the unbalanced network state using a generalized model," *IEEE Trans. Power Electron.*, vol. 11, no. 3, pp. 495–502, May 1996.

[11] A. Yazdani and R. Iravani, "A unified dynamic model and control for the voltage-sourced converter under unbalanced grid conditions," *IEEE Trans. Power Del.*, vol. 21, no. 3, pp. 1620–1629, Jul. 2006.

[12] Y. Jiang and A. Ekstrom, "Applying PWM to control overcurrents at unbalanced faults of forced-commutated VSCs used as static VAr compensators," *IEEE Trans. Power. Del.*, vol. 12, no. 1, pp. 273–278, Jan. 1997.

[13] S. E. M. de Oliveira and J. O. R. Guimaraes, "Effects of voltage supply unbalance on AC harmonic current components produced by AC/DC converters," *IEEE Trans. Power Del.*, vol. 22, no. 4, pp. 2498–2507, Oct. 2007.

[14] C. Hochgraf and R. H. Lasseter, "Statcom controls for operation with unbalanced voltages," *IEEE Trans. Power Del.*, vol. 13, no. 2, pp. 538–544, Apr. 1998.

[15] M. Saeedifard, H. Nikkhajoei, and R. Iravani, "A space vector modulated STATCOM based on a three-level neutral point clamped converter," *IEEE Trans. Power Del.*, vol. 22, no. 2, pp. 1029–1039, Apr. 2007.

[16] N. C. Sahoo, B. K. Panigrahi, P. K. Dash, and G. Panda, "Application of a multivariable feedback linearization scheme for STATCOM control," *Elect. Power Syst. Res.*, vol. 62, pp. 81–91, Jun. 2002.

[17] Q. Song, W. Liu, and Z. Yuan, "Multilevel optimal modulation and dynamic control strategies for STATCOMs using cascaded multilevel inverters," *IEEE Trans. Power Del.*, vol. 22, no. 3, pp. 1937–1946, Jul. 2007.

[18] G. E. Valderrama, P. Mattavelli, and A. M. Stankovic, "Reactive power and imbalance compensation using STATCOM with dissipativity-based control," *IEEE Trans. Control Syst. Technol.*, vol. 9, pp. 718–727, Sep. 2001.

[19] G. Escobar, A. M. Stankovic, and P. Mattavelli, "An adaptive controller in stationary reference frame for D-statcom in unbalanced operation," *IEEE Trans. Ind. Electron.*, vol. 51, no. 2, pp. 401–409, Apr. 2004.

[20] A. Jain, K. Joshi, A. Behal, and N. Mohan, "Voltage regulation with STATCOMs: modeling, control and results," *IEEE Trans. Power Del.*, vol. 21, no. 2, pp. 726–735, Apr. 2006.

[21] S. Chen, G. Joos, and L. T. Moran, "Dynamic performance of PWM STATCOMs operating under unbalance and fault conditions in distribution systems," *Proc. IEEE Power Eng. Soc. Winter Meeting*, vol. 2, pp. 950–955, Jan. 2001.

[22] L. Xu, B. R. Andersen, and P. Cartwright, "Control of VSC transmission systems under unbalanced network conditions," *Proc. IEEE Power Eng. Soc. Transmission and Distribution Conf. Expo.*, vol. 2, pp. 626–632, Sep. 2003.

[23] Y. Suh and T. A. Lipo, "Control scheme in hybrid synchronous stationary frame for PWM AC/DC converter under generalized unbalanced operating conditions," *IEEE Trans. Ind. Appl.*, vol. 42, no. 3, pp. 825–835, May/Jun. 2006.

[24] A. M. Stankovic, H. Lev-Ari, and M. M. Perisic, "Analysis and implementation of model-based linear estimation of dynamic phasors," *IEEE Trans. Power Syst.*, vol. 19, no. 4, pp. 1903–1910, Nov. 2004.
[25] A. A. Girgis, W. Chang, and E. B. Makram, "Analysis of high-impedance fault generated signals using a kalman filtering approach," *IEEE Trans. Power Del.*, vol. 5, no. 4, pp. 1714–1724, Oct. 1990.
[26] R. A. Flores, I. Y. H. Gu, and M. H. J. Bollen, "Positive and negative sequence estimation for unbalanced voltage dips," *Proc. IEEE Power Eng. Soc. General Meeting*, vol. 4, pp. 2498–2502, Jul. 2003.
[27] P. W. Lehn and M. R. Iravani, "Discrete time modeling and control of the voltage source converter for improved disturbance rejection," *IEEE Trans. Power Electron.*, vol. 14, no. 6, pp. 1028–1036, Nov. 1999.
[28] H.-S. Song, I.-W. Joo, and K. Nam, "Source voltage sensorless estimation scheme for PWM rectifiers under unbalanced conditions," *IEEE Trans. Ind. Electron.*, vol. 50, no. 6, pp. 1238–1245, Dec. 2003.
[29] M. K. Mishra, A. Ghosh, A. Joshi, and H. M. Suryawanshi, "A novel method of load compensation under unbalanced and distorted voltages," *IEEE Trans. Power Del.*, vol. 22, no. 1, pp. 288–295, Jan. 2007.
[30] Y. Suh, V. Tijeras, and T. A. Lipo, "A nonlinear control of the instantaneous power in dq synchronous frame for PWM AC/DC converter under generalized unbalanced operating conditions," in *Proc. 37th IAS Annu. Meeting*, Oct. 2002, vol. 2, pp. 1189–1196.
[31] V. Blasco and V. Kaura, "A new mathematical model and control of a three-phase AC-DC voltage source converter," *IEEE Trans. Power Electron.*, vol. 12, no. 1, pp. 116–123, Jan. 1997.
[32] K. Ogata, *Modern Control Engineering*, 3rd ed. Englewood Cliffs, NJ: Prentice-Hall, 1997.
[33] H. Yoo, J.-H. Kim, and S.-K. Sul, "Sensorless operation of a PWM rectifier for a distributed generation," *IEEE Trans. Power Electron.*, vol. 22, no. 3, pp. 1014–1018, May 2007.
[34] I. Agirman and V. Blasko, "A novel control method of a VSC without AC line voltage sensors," *IEEE Trans. Ind. Appl.*, vol. 39, no. 2, pp. 519–524, Mar./Apr. 2003.
[35] H.-S. Song and K. Nam, "Dual current control scheme for PWM converter under unbalanced input voltage conditions," *IEEE Trans. Ind. Electron.*, vol. 46, no. 5, pp. 953–959, Oct. 1999.
[36] F. Esfandiari and H. K. Khalil, "Output feedback stabilization of fully linearizable systems," *Int. J. Control*, vol. 56, pp. 1007–1037, 1992.
[37] A. Teel and L. Praly, "Tools for semi-global stabilization by partial state output feedback," *SIAM J. Control Optim.*, vol. 22, pp. 1443–1488, 1995.
[38] M. Etchechoury, J. Solsona, and C. Muravchik, "On the stability of nonlinear plants that include an observer for their feedback linearization," *Int. J. Syst. Sci.*, vol. 27, pp. 1461–1466, 1996.
[39] M. Etchechoury, J. Solsona, and C. Muravchik, "Feedback linearization via state transformation using estimated states," *Int. J. Syst. Sci.*, vol. 32, no. 1, pp. 1–7, 2001.
[40] H. Akagi, Y. Kanazawa, and A. Nabae, "Instantaneous reactive power compensators comprising switching devices without energy storage components," *IEEE Trans. Ind. Appl.*, vol. IA-20, no. 3, pp. 625–630, May 1984.

Andres E. Leon (S'05) was born in Argentina in 1979. He received the electrical engineering degree from the National University of Comahue, Neuquén, Argentina, in 2005 and is currently pursuing the Ph.D. degree in control systems at the Instituto de Investigaciones en Ingeniería Eléctrica "Alfredo Desages" (IIIE), Universidad Nacional del Sur, Bahía Blanca, Argentina.

His primary areas of interest are power systems control, custom power systems, and wind energy conversion systems.

Juan Manuel Mauricio (S'04) was born in Argentina in 1977. He received the electrical engineering degree from the National University of Comahue, Neuquén, Argentina, in 2003, and is currently pursuing the Ph.D. degree in electrical engineering at the University of Seville, Seville, Spain.

His primary areas of interest are power systems modeling and control and flexible ac transmission systems.

Jorge A. Solsona (SM'04) received the electronics engineer and Dr. degrees from the Universidad Nacional de La Plata, La Plata, Argentina, in 1986 and 1995, respectively.

Currently, he is with the Instituto de Investigaciones en Ingeniería Eléctrica Alfredo Desages (IIIE), Departamento de Ingeniería Eléctrica y de Computadoras, Universidad Nacional del Sur, Bahía Blanca, Argentina, and CONICET where he is involved in teaching and research on control theory and its applications in electromechanical systems.

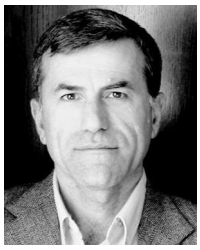

Antonio Gomez-Exposito (F'05) was born in Spain in 1957. He received the electrical and D.Eng. degrees from the University of Seville, Seville, Spain, in 1982 and 1985, respectively.

Since 1982, he has been with the Department of Electrical Engineering, University of Seville, where he is currently a Professor and Chairman of the Department. His primary areas of interest are power system optimization, state estimation, and digital signal processing.